Steel and Composite Structures, Vol. 10, No. 1 (2010) 23-43
DOI: http://dx.doi.org/10.12989/scs.2010.10.1.023

Modelling of beam-to-column connections at elevated temperature using the component method

N.H. Ramli Sulong[1*], A.Y. Elghazouli[2†], B.A. Izzuddin[2‡] and N. Ajit[1‡†]

[1]*Department of Civil Engineering, University of Malaya, 50603 Kuala Lumpur, Malaysia*
[2]*Department of Civil and Environmental Engineering, Imperial College London, SW7 2BU, UK*

(Received August 28, 2009, Accepted November 24, 2009)

Abstract. In this paper, a nonlinear model is developed using the component method in order to represent the response of steel connections under various loading conditions and temperature variations. The model is capable of depicting the behaviour of a number of typical connection types including endplate forms (extended and flush) and angle configurations (double web, top and seat, and combined top-seat-web) in both steel and composite framed structures. The implementation is undertaken within the finite element program ADAPTIC, which accounts for material and geometric nonlinearities. Verification of the proposed connection model is carried out by comparing analytical simulations with available results of isolated joint tests for the ambient case, and isolated joint as well as sub-frame tests for elevated temperature conditions. The findings illustrate the reliability and efficiency of the proposed model in capturing the stiffness and strength properties of connections, hence highlighting the adequacy of the component approach in simulating the overall joint behaviour at elevated temperature.

Keywords : beam-to-column connections; elevated temperature; non-linear finite element analysis; component method.

1 Introduction

Experimental studies, such as the full-scale fire tests carried out in Cardington (e.g. O'Connor, *et al*. 2003; Bailey, *et al*. 1999), have shown that steel connections can have a significant influence on the fire performance of steel-framed structures. Understanding the behaviour of steel joints under fire conditions is vital for addressing performance-based design procedures (e.g. EN1993:1-8 2005) in a reliable manner.

Detailed investigations dealing with the response of steel connections at elevated temperature are increasing (e.g. Simoes da Silva, *et al*. 2005), and various connection types have been experimentally examined. For example, Lawson (1990) tested endplate and cleat connections under fire, followed by Leston-Jones, *et al*. (1997). Spyrou, *et al*. (2004a and 2004b) focused more on T-stub components. Other researchers also tested endplate connections, including Al-Jabri, *et al*. (2005), Wang, *et al*. (2007)

*Corresponding Author, E-mail: hafizah_ramli@um.edu.my
†E-mail: a.elghazouli@imperial.ac.uk
‡E-mail: b.izzuddin@imperial.ac.uk
‡†E-mail: norainiajit@yahoo.com

and Qian, *et al*. (2008). On the other hand, limited studies on angle connections are available (Hongxia, *et al*. 2009a; Saedi Daryan and Yahyai 2009). Additionally, fin-plate connections were experimentally examined by Hongxia, *et al*. (2009b). Apart from isolated connections, steel sub-frame tests focusing on endplate connections have been reported (Santiago, *et al*. 2009).

There is a limit on the range and number of specimens that can be experimentally investigated under fire conditions due to cost and practical restrictions. Accordingly, there is a need for reliable analytical approaches that can represent the behaviour of connections at elevated temperature in order to permit parametric and design assessments. In this context, the component-based approach offers several merits in terms of accuracy and relative ease of application. Simoes da Silva, *et al*. (2001) examined the response of flush end plate connections at elevated temperature based on modifications to the moment-rotation curve of the connections at ambient temperature. Spyrou, *et al*. (2004a and 2004b) investigated the individual component behaviour in the tension and compression zone of endplate connections. Al-Jabri, *et al*. (2005) developed a component-based model for flexible endplate connections in steel and composite joints. Wang, *et al*. (2007) predicted the response of extended endplate connections with and without column stiffeners based on the recommendations presented in the Chinese Technical Code on Fire Safety of Steel Buildings. Block, *et al*. (2007) focused on the compression zone of endplate connections. Combining the tension zone model by Spyrou, *et al*. (2004b), the complete endplate component-based procedure was incorporated into the finite element program Vulcan. Qian, *et al*. (2009) also investigated endplate connections and incorporated the beam web shear component together with existing tension and compression zone components. Hongxia, *et al*. (2009a) developed a model focusing on the behaviour of angles up to fracture, for a web cleat connection.

All previous studies on the component-based approach have provided reasonable estimates for the initial stiffness and moment resistance of the specific connection type considered. Some models are capable of producing non-linear response curves and can predict the behaviour up to component failure (e.g. Hongxia, *et al*. 2009a). However, each model focuses on a specific connection type and not all models can incorporate the full response under natural fire scenarios.

The aim of this paper is to describe the development of a component-based approach for five connection types including endplate forms (extended and flush) and angle configurations (double web, top and seat, and combined top, seat-web angle) in both steel and composite framed structures. The model is capable of representing the connection response under ambient and elevated temperature, as well as generalized loading conditions including possible load reversals. The connection model is implemented within the nonlinear finite element program ADAPTIC (Izzuddin 1991). Verification studies on various connection configurations at ambient as well as at elevated temperature, are carried out in order to verify the accuracy and reliability of the model.

2 Connection modelling

2.1 General approaches

The component-based method considers any joint as a set of individual basic components. An accurate joint representation requires a consideration of all possible components at each bolt-row along its depth in order to account for the effect of combined axial-moment loading. A single model accounting for various conditions that exist in joints such as strain reversal and the redistribution of internal forces at ambient and elevated temperature is described herein. The proposed model is not restricted to steel connections only, but could also be extended to composite joints (Ramli Sulong 2005). However, in this paper, the verification section focuses only on steel joints.

2.1.1 Joint characterisation

The constituent connection components should be selected to represent closely the expected behaviour depending on the applied loading conditions. The proposed connection model considers that these components can be subjected to either tension or compression. In tension zones, active components may vary depending on their geometry and location. For the compression zones, the column web in compression contributes to the behaviour of a connection as agreed in previous studies (Spyrou, *et al*. 2004a, Al-Jabri, *et al*. 2005). On the other hand, for the shear panel, the column web governs the connection behaviour; this component is only activated when unbalanced moments exist in the connection, and is considered herein as a separate component acting in series with the connection element.

Fig. 1 provides an illustration of a simplified mechanical model for typical endplate and angle connections. Currently, three active components are used for the endplate connections and seven active components to represent angle connections.

For all components, idealised tri-linear force-deformation relationships are formulated. In developing the cyclic response of the force-deformation curve of a component, the classic Massing rule is adopted for the construction of the unloading and reloading paths. This is to account for the strain reversal due to load redistribution or due to heating and cooling. The same approach is adopted by El-Rimawi, *et al*. (1996), Bailey, *et al*. (1996) and Block, *et al*. (2007) in their models.

2.1.2 Elevated temperature effects

Due to the influence on material properties, connections subjected to elevated temperature can exhibit significant reduction in stiffness and strength. Hence, parameters such as the elastic modulus as well as yield and ultimate stress, need to account for the expected degradation with increasing temperature. Strength Reduction Factors (SRF) at strain levels corresponding to the proportional limit and 1.0% (Al-Jabri, *et al*., 2004) are adopted for the reduction in stiffness and strength, respectively for all components. On the other hand, for bolt properties, the relationships proposed by Kirby (1995) are used to find the strength of a bolt at a certain temperature, whilst the reduction in stiffness is based on the recommendations of Al-Jabri, *et al*. (2004). It should be noted that the temperature-dependant properties in the developed model are user defined and can be modified if necessary. However, the effect of thermal expansion within the connection components is not included in this study due to the lack of data in the literature on the actual thermal expansion of each component. The model also

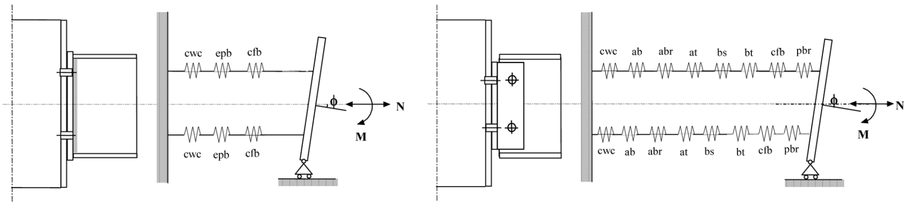

(a) Endplate connection (b) Angle connection

Fig. 1 Nonlinear spring connection model enables a quadratic temperature distribution throughout the joint depth, and individual temperatures can be applied to each component in a bolt row.

2.2 End plate connections

For extended and flush endplate connections, T-stub elements are traditionally used to represent the components in the tension zone. This is implemented by adopting appropriate orientation of the idealised T-stub components in order to account for the deformation due to the column flange as well as the endplate in bending.

2.2.1 T-stub idealisation

The active components which are represented by T-stubs are the endplate in bending, column flange in bending and bolts in tension. Plastic beam analysis is applied to analyse a T-stub in tension. The force diagram in the T-stub is presented in Fig. 2. Three modes of failure can be observed (EN1993-1-8 2005), as shown in Fig. 3.

The corresponding component strength for these failure modes, together with the computation of the effective width, is based on EN1993-1-8 (2005). However for this study, the case of individual bolt-rows is considered at present. The rotational stiffness of the joint is calculated based on the resultant stiffness of individual components. For a row with 2 bolts in tension, assuming that the bolts are subjected to a direct tensile force in isolation, the axial stiffness for each bolt row, K_{bt}, can be calculated based on the principles of Hooke's law, such that:

$$K_{bt} = \frac{1.6 E_b A_b}{L_b} \tag{1}$$

where E_b is the bolt elastic modulus, A_b is the bolt shank effective cross-section area and L_b is the effective length of the bolt according to EN1993-1-8 (2005). The coefficient 1.6 is considered (Weynand, *et al*. 1995) due to the influence of prying forces which produces an increase in the bolt axial force. For the column flange (K_{cfb}) and endplate in bending (K_{epb}), the stiffness relationships are:

$$K_{cfb} = \frac{0.9 L_{eff} t_{cf}^3}{m^3} \tag{2}$$

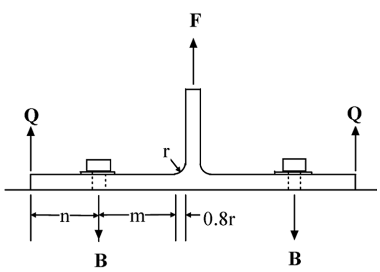

Fig. 2 Force diagram of T-stub components

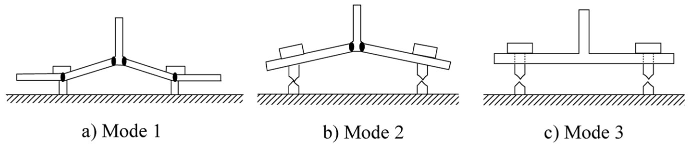

Fig. 3 Failure modes of a T-stub

$$K_{epb} = \frac{0.9L_{eff}t_{ep}^3}{m^3} \tag{3}$$

where L_{eff} is the effective length of each row taken from EN1993-1-8 (2005), t_{cf} and t_{ep} are the thicknesses of the column flange and endplate, respectively, and m is the distance from the bolt centreline to the flange-to-web root radius. The effect of bolt preloading on the rotational stiffness of the connection can be included by multiplying the coefficient which accounts for the restraint condition and the reduction of the flange span due to bolt action, ψ, with the elastic stiffness of the column flange and endplate in bending. Based on Faella, *et al*. (2000b), the coefficient ψ is given as:

$$\psi = \left(\frac{t_{cf}}{d_b\sqrt{\alpha}}\right)^{-1.28} \tag{4}$$

where d_b is the bolt diameter and $\alpha = m/d_b$.

2.3 Connections with angles

2.3.1 Main assumptions

Three types of bolted angle connections are considered, namely double web angles, top and seat angles and combined top-seat-web angles. Modelling of connections with angles can be carried out by considering the whole depth of a connection as consisting of a number of layers. For the double web angles, the number of layers is assumed to be the same as the number of bolt rows. For the top and seat angles, the whole angle section (top or seat) is considered as a single layer. It is assumed that each connection layer acts independently and resistance to moment can be considered as the summation of resistances within each segment.

Experimental results (e.g. Shen and Astaneh-Asl 1999) indicate that when an angle segment is subjected to tension beyond the yield force of the component, plastic hinges are observed near the fillet of each leg and near the location of the column bolts as shown in Fig. 4. To account for the failure modes of angle connections, seven active components have been identified in the tension zone: bolts in tension/shear, column flange in bending, beam web/flange in bearing, web/top/seat angle in bearing/ bending/ tension. At this stage, it is considered that there is no interaction between the components, and that their strength is calculated based on the component behaviour in isolation.

2.3.2 Response parameters

a. Component strength

1) Bolts in tension, F_{bt}

When a layer is subjected to a tensile force, the bolt connected to the column leg (i.e. leg connected to column flange, as shown in Fig. 4 is subjected to tension. For two bolts in tension (with yield stress of f_{yb}), the axial force is calculated as:

$$F_{bt} = 2f_{yb}A_b \tag{5}$$

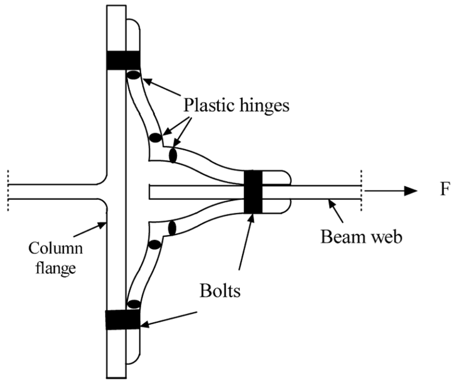

Fig. 4 Deformed shape of angle connection

2) Bolts in shear, F_{bs}

For the bolts connecting the double angles back-to-back and for both top/seat angles connected to the beam tension/compression flange, the resistance in shear is given as:

$$F_{bs} = n_b 0.6 f_{ub} A_b \tag{6}$$

where n_b is the number of bolts and f_{ub} is the bolt material ultimate stress.

3) Column flange in bending, F_{cfb}

This case is the same as that presented before for the equivalent T-stub.

4) Beam web/flange in bearing, F_{pbr}

In the tension zone, the beam web or flange is subjected to shear when the bolt shank acts in bearing against the bolt-hole walls. In this study, formulation of beam web or flange in bearing is based on empirical formula (Faella, *et al.* 2000b) and is given as:

$$F_{pbr} = 2.5\alpha f_{yp} d_b t_p \tag{7}$$

where f_{yp} is the yield stress of the beam web/flange, t_p is thickness of beam web/flange and α for both beam web and flange in bearing is taken as the minimum of:

$$\alpha = \min\left\{\frac{e_b}{3d_0};\frac{p_b}{3d_0}-\frac{1}{4};\frac{f_{ub}}{f_{up}};1\right\} \tag{8}$$

where e_b is the distance from the bolt line to the free edge in the direction of applied force, p_b is the spacing between bolts, d_b and d_0 are the bolt diameter and bolt hole diameter, respectively, f_{ub} and f_{up} are the ultimate strength of bolt and beam web/flange, respectively.

5) Angle in bearing, F_{abr}

A similar formulation to that of the beam web/flange in bearing is adopted (Eq. (7)).

6) Angle in bending, F_{ab}

The angle in bending for the double web angles is modelled for each bolt-row. On the other hand, for the top and seat angles, the equivalent T-stub as suggested in EN1993-1-8 (2005) is adopted as shown in Fig. 5. The angle connected to the column flange (column leg) is subjected to bending. Accordingly, when four plastic hinges form at the bolt lines and near the fillet of the column legs, the force F for the double angles in each bolt-row (or the equivalent T-stub for the top and seat angles) can be calculated as:

$$F = \frac{L_{eff} t_a^2 f_{ya}}{m} \tag{9}$$

where L_{eff} is the effective length of the angle determined in the same manner as for the T-stub flange (EN1993-1-8 2005) for the double web angles. For the case of top and seat angles, L_{eff} is taken as half of the angle length as shown in Fig. 5 since the bolts are normally closely spaced; t_a is the angle thickness and f_{ya} is the yield stress of the angle, whilst m is the distance between the two hinges in each column leg.

7) Angle in tension, F_{at}

For the angle leg connected to the beam (beam web for web angle or beam flange for top/seat angle), the capacity of the angle leg in tension is calculated as:

$$F_{at} = L_{eff} t_a f_{ya} \tag{10}$$

It should be noted that the effective length of the angle segment in the beam leg is idealised to be similar to the effective length in the column leg (same as the effective length in the T-stub flange (EN1993-1-8 2005).

b. Component stiffness

1) Bolts in tension, K_{bt}

For each bolt row, the initial stiffness of the bolts in tension is determined in the same manner as that of the endplate connection as given in Eq. (1) before.

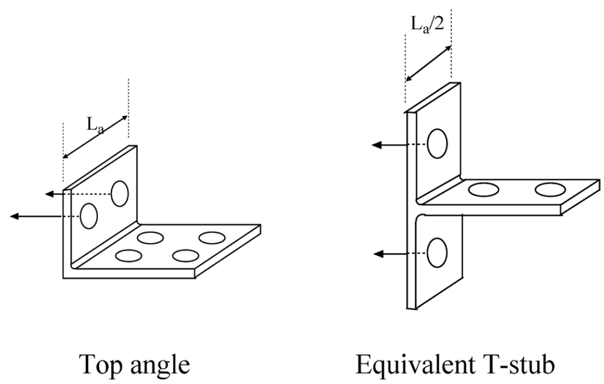

Fig. 5 Equivalent T-stub model for the top angle in bending (EN1993-1-8 2005)

2) Bolts in shear, K_{bs}

For bolts in shear, the flexibility of the angle connection is accounted for. The stiffness of two snug-tightened bolts in a single bolt row is given as:

$$K_{bs} = \frac{16 d_b^2 f_{ub}}{d_{M16}} \tag{11}$$

where d_{M16} is the diameter of M16 bolt. The above formulation is applied to the case of snug tightened bolts. In the case of preloaded bolts, the stiffness is considered to be infinite.

3) Column flange in bending, K_{cfb}

Similar to endplate connections, calculation of the stiffness of the column flange in bending is based on an equivalent cantilever model as given in Eq. (2).

4) Beam web/flange in bearing, K_{pbr}

The stiffness of plates (beam web/flange) in bearing, for non-preloaded bolts, based on Faella, *et al.* (2000b) is given as:

$$K_{pbr} = 24 k_a k_b d_b f_{up} \tag{12}$$

where k_a and k_b are parameters defined as follows:

$$k_a = \min\left\{1.5\frac{t_p}{d_{M16}};2.5\right\} \tag{13}$$

$$k_b = \min\left\{0.25\frac{e_b}{d_b} + 0.5;0.25\frac{p_b}{d_b} + 0.375;1.25\right\} \tag{14}$$

5) Angle in bearing, K_{abr}

This is similar to the stiffness of the beam web/flange in bearing (Eq. (12)-(14)).

6) Angle in bending, K_{ab}

Using an equivalent cantilever model, similar to the column flange in bending (described in Section 2.2.1), the stiffness for the double angles in bending in each bolt-row as well as for the top or seat angle follows the same T-stub idealisation described before.

7) Angle in tension, K_{at}

The procedure used for the angle in tension is applied to the angle leg connected to the beam web for double angle connection and angle leg connected to beam flange for the case of top/seat angle. The component is considered as a bar of width L_{eff} and depth t_a, determined as:

$$K_{at} = \frac{EL_{eff}t_a}{g_{bl}} \tag{15}$$

The same effective length L_{eff} adopted for capacity estimation in web or top/seat angles is used in calculating the stiffness; g_{bl} is the gauge length of the angle beam leg.

2.4 Treatment of compression zone

In this study, only the column web is considered to represent the flexibility of the compression zone in an unstiffened connection (Spyrou, *et al*. 2004a; Al-Jabri, *et al*. 2005; Block, *et al*. 2007). For stiffened connections, the column web is assumed to be rigid. Similar to the components in tension, the column web in compression is determined for each bolt-row to account for the possible effect of cyclic loading in the joint. The strength of the column web in compression when first yielding occurs is:

$$F_{cwc1} = L_{eff} t_{cw} f_{ycw} \tag{16}$$

where f_{ycw} is the yield stress of the column web, t_{cw} is the column web thickness, and L_{eff} is the effective width of the column web in compression transmitted by the connection. For flush and extended endplate connections, the effective width is equal to the depth of the endplate divided by the number of bolt rows. For partial depth endplate and double web angle connections, the effective width of the inner bolt-rows is equal to the bolt spacing. For the outermost bolt-row, taking into consideration the possibility that the beam flange might exert a compression force on the column web at large displacement, the effective length for these layers is approximately equal to:

$$L_{eff} = \frac{h_b - p_b(n-2)}{2} \tag{17}$$

where h_b is the beam height, p_b is the bolt pitch and n is the number of bolt-row. For the top and seat angles, the effective length of the column web in compression is based on EN1993-1-8 (2005) as follows:

$$L_{eff} = (2t_a + 0.6r_a + 5(t_{fc} + r_c)) \tag{18}$$

where r_a and r_c are the angle and column radii, respectively. Subsequent to the onset of plasticity, the ultimate capacity of the column web can be determined by substituting the yield stress with the ultimate stress in Eq. (16). The initial stiffness of the column web in compression, K_{ecwc} can be considered as:

$$K_{ecwc} = E\frac{L_{eff}t_{cw}}{d_{cw}} \tag{19}$$

where d_{cw} is the clear depth of the column web. Similar effective length, L_{eff}, as in the calculations of the strength of the component is applied for the estimation of stiffness.

For the post yield hardening, a strain hardening stiffness K_{pcwc} is determined as:

$$K_{pcwc} = \mu K_{ecwc} \tag{20}$$

where μ is the strain hardening coefficient.

2.5 Shear panel

The shear deformation of the panel zone contributes to the joint flexibility and may need to be incorporated in the modelling of the joint. The model proposed by Krawinkler, *et al*. (1975) provides a reliable formulation in predicting the shear-deformation behaviour of the panel zone and thus is considered in this study. Activation of the shear panel deformation depends on the configuration of the structure and the location of the connection. In the case of single sided joints, this component is considered as a spring connected in series with the modelled connection element. The spring representing the shear panel is an existing joint element in ADAPTIC (Izzuddin 1991), where tri-linear force-deformation or moment-rotation relationship with cyclic loading is considered.

3. Overall joint response

3.1 Component force-deformation response

An idealised tri-linear model is used to represent the component response for monotonic loading both at ambient and elevated temperature, as shown in Fig. 6. The first slope represents the elastic stiffness up to the attainment of yield strength. The second slope is determined by using the same equations in Section 2, but in terms of the tangent modulus and the ultimate material strength. The third slope is obtained by multiplying the initial stiffness with a reduced hardening coefficient (approximately $E_u/E_e = 0.2\%$ for S275 steel) considering the true stress-strain relationship (Faella, *et al*. 2000b).

Under fire conditions, structural members and components may be subjected to load reversals. Mathematical models based on the classic Massing rule are normally adopted to define the rules of loading and unloading paths as it is widely used for modelling stress-strain curves of steel and concrete. Knowing the critical points for forces and stiffness of the component at each level of temperature, the cyclic force-deformation curve can be constructed. The cyclic curves for the components in tension and compression under a specific temperature, T, are illustrated in Fig. 7.

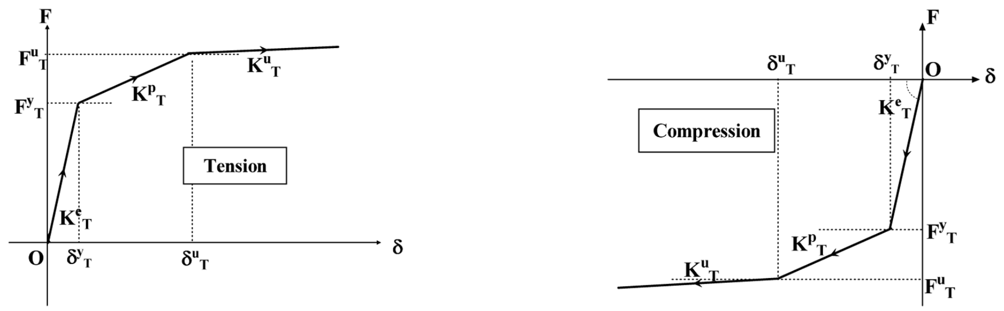

Fig. 6 Monotonic force-displacement curve for components in tension and compression

3.2 Derivation of nonlinear relationships and implementation procedures

The iterative procedure to develop the whole non-linear moment-rotation curve is implemented within the advanced finite element program ADAPTIC (Izzuddin 1991). The computer code for the connection model was written in FORTRAN. After testing it in an independent mode, it was then implemented in ADAPTIC, by developing a new 3D element for the joint, referred to as 'jbc2'. This element consists of two coincident nodes prior to loading plus a third node to determine the beam direction.

In the non-linear procedure, firstly the updated geometric configuration of the connection element is established. The freedom number is obtained and the direction cosine of the joint as well as it local displacement is determined. Based on the reference origin at mid-height of the connection, the depth of each layer is determined. This is followed by the computation of the layer temperature and the material properties corresponding to this temperature. In each layer, for connections subjected to combined axial force and bending moment, the layer displacement δ_i is calculated, and is given as:

$$\delta_i = u - \phi y_i \tag{21}$$

where u and ϕ are the horizontal displacement and rotation, respectively, whilst y_i is the distance of the layer i to the beam mid-depth. For a layer deformation, δ_i, the force f_i is obtained from the nonlinear load-deformation curve of the weakest component in each layer. The components are arranged in the order of yielding. The layer force is summed up to obtain the total connection axial force N and consequently the connection moment M, for n number of layers, as follows:

$$N = \sum_{i=1}^{n} f(\delta_i) \tag{22}$$

$$M = -\sum_{i=1}^{n} f(\delta_i) y_i \tag{23}$$

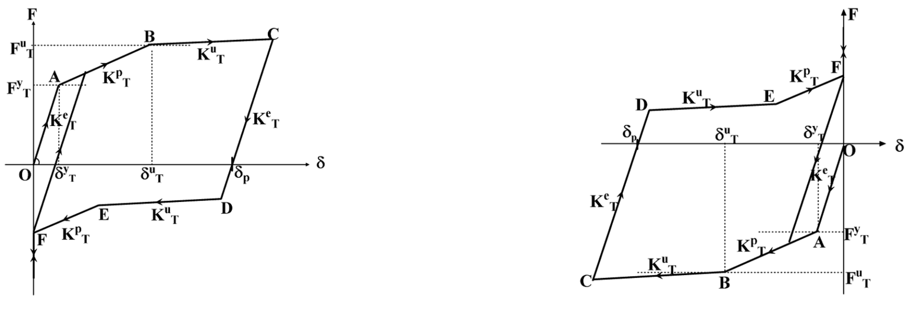

(a) Tension (b) Compression

Fig. 7 Tri-linear cyclic force-displacement relationships for components

The connection stiffness matrix, K is calculated by summation of the layer stiffness:

$$[K] = \begin{bmatrix} \left(\frac{\partial N}{\partial u}\right) & \left(\frac{\partial N}{\partial \phi}\right) \\ \left(\frac{\partial M}{\partial u}\right) & \left(\frac{\partial M}{\partial \phi}\right) \end{bmatrix} \tag{24}$$

$$\left(\frac{\partial N}{\partial u}\right) = \sum_{i=1}^{n} K_i \tag{25}$$

$$\left(\frac{\partial N}{\partial \phi}\right) = \left(\frac{\partial M}{\partial u}\right) = \sum_{i=1}^{n} K_i y_i \tag{26}$$

$$\left(\frac{\partial M}{\partial \phi}\right) = \sum_{i=1}^{n} K_i y_i^2 \tag{27}$$

where K_i is the tangent stiffness of the connection layer i, obtained from the summation of the spring stiffness in series for each layer.

4. Validation studies

4.1 Ambient response

The proposed model was validated against the results of several experimental studies for five connection types. It is acknowledged that there is extensive experimental data in the literature on steel connection response at ambient temperature, but selected results are shown here, as more focus is given to the elevated temperature case. These include T-stub components (Faella, *et al*. 2000a; Spyrou, *et al*. 2004b), flush endplate connections (Simoes da Silva, *et al.* 2004; Leston-Jones, *et al.* 1997), extended endplate configurations (De Lima, *et al*. 2004; Girao Coelho, *et al*. 2004), double web angles (Davison, *et al*. 1987; Yang and Lee 2007), top and seat angles (Shen and Astaneh 1999; Azizinamini 1982; Komuro, *et al*. 2004) and combination of top, seat and web angles (Azizinamini, *et al*. 1987). Further validation for connections in composite floors can be found elsewhere (Ramli Sulong 2005; Ramli Sulong, *et al*. 2007).

Comparisons between the numerical simulations and test results are shown in Figs. 8 to 13. In general, it is shown that the model can provide a close prediction of the load-deformation/ moment-rotation curves obtained from the tests. Table 1 summarizes the comparison of the numerical and experimental results in terms of initial stiffness and capacity. Depending on the experimental parameters considered (i.e. M-θ curve or F-δ curve), the initial stiffness is either related to rotational or axial stiffness. For the resistance, it can be either force or moment resistance. This value is measured at the point where the initial slope of the curve intersects with the stiffness in the plastic region. The percentage error, mean error and its standard deviation are also shown in the table.

It is evident from the comparisons that the resistance is predicted within a narrow error margin (with a mean error of 0.5%). However, the initial stiffness is overestimated especially for top-seat angle (Azizinamini-A1) and combined top-seat-web angle (Azizinamini, *et al*.-8S1 and 8S2). These discrepancies particularly for angle connections are due to bolt slippage/bolt pretension, residual stresses and imperfections

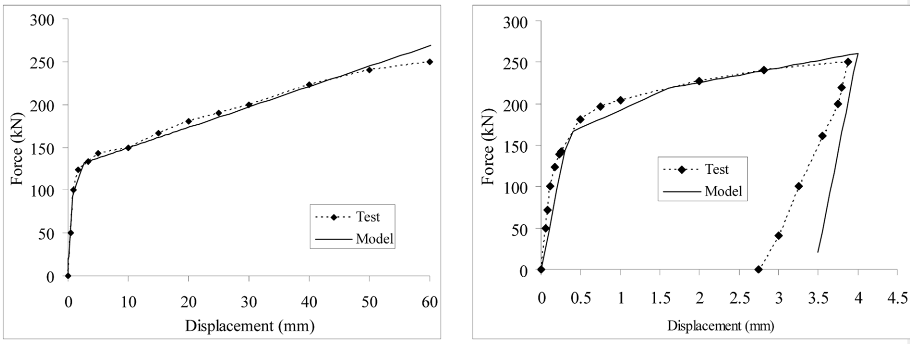

(a) Faella, *et al.* (2000b) test (b) Spyrou, *et al.* (2004b) test- AB1

Fig. 8 T-stub at ambient temperature

Table 1 Comparison between numerical and experimental results for the prediction of initial stiffness and capacity at ambient temperature

Connection	Author	Initial stiffness			Force / Moment resistance		
		Numerical (kN/mm)	Experimental (kN/mm)	% error	Numerical (kN)	Experimental (kN)	% error
T-stub	Faella, *et al.*	122.27	113.64	–7.59	128.41	128.77	0.28
	Spyrou, *et al.* -AB1	480.00	569.24	15.68	198.17	193.26	–2.54
Top-seat angle	Shen and Astaneh	156.75	156.67	0.00	117.50	107.96	–8.83
		Numerical (kNm/rad)	Experimental (kNm/rad)	% error	Numerical (kNm)	Experimental (kNm)	% error
Flush endplate	Simoes da Silva, *et al.*	16327.08	16345.18	0.11	71.69	72.75	1.46
	Leston-Jones, *et al.*	3833.33	2400.00	–59.72	14.39	15.54	7.38
Extended endplate	De Lima, *et al.*	37220.93	36236.93	–2.72	119.35	112.72	–5.88
	Girao Coelho, *et al.*	38187.50	34660.00	–10.18	103.37	96.00	–7.67
Double web angle	Davison, *et al.*	1220.00	2200.00	44.55	4.92	4.32	–13.86
	Yang and Lee	8111.05	8052.00	–0.73	20.89	24.00	12.95
Top-seat angle	Azizinamini - A1	45351.47	17857.14	–153.97	41.43	47.32	12.46
	Azizinamini - A2	47830.19	45720.00	–4.62	50.77	58.13	12.67
	Kumoro, *et al.*	54798.76	54799.51	0.00	66.00	62.70	–5.26
Top-seat-web angle	Azizinamini, *et al.* - 8S1	17000.00	8333.33	–104.00	26.25	26.18	–0.27
	Azizinamini, *et al.* - 8S2	20000.00	11000.00	–81.82	44.60	42.25	–5.56
	Azizinamini, *et al.* - 8S9	14450.00	14800.00	2.36	39.43	37.51	–5.12
Mean error				–24.18			–0.52
Standard deviation				50.984			8.129

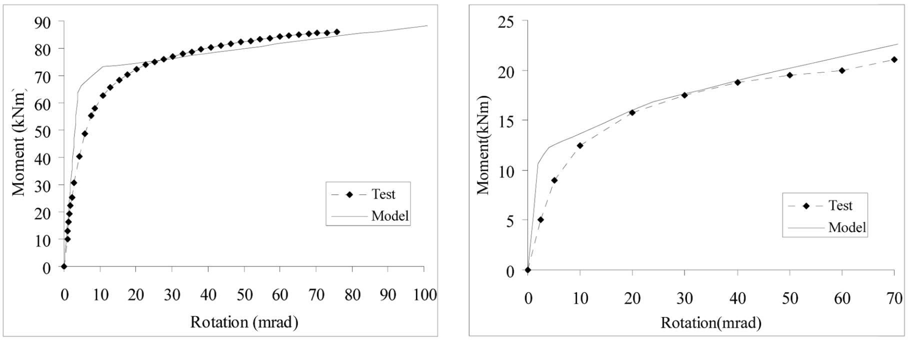

(a) Simoes da Silva, *et al.* 2004 test (b) Leston-Jones, *et al.* 1997 test

Fig. 9 Flush endplate connection at ambient temperature

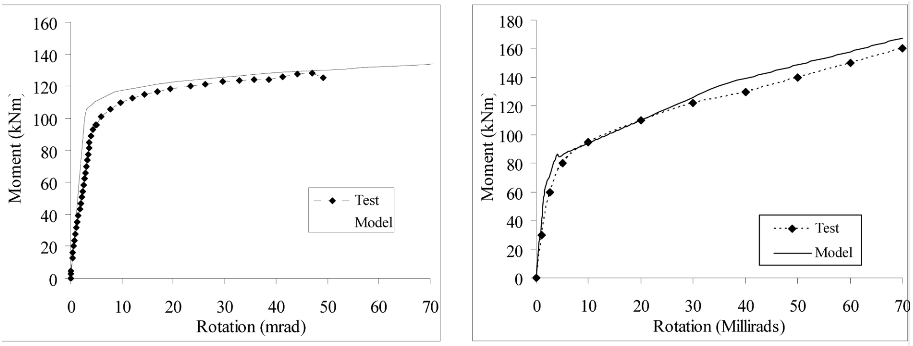

(a) De Lima, *et al.* 2004 test (b) Girao Coelho, *et al.* 2004 test- FS1

Fig. 10 Extended endplate connection at ambient temperature

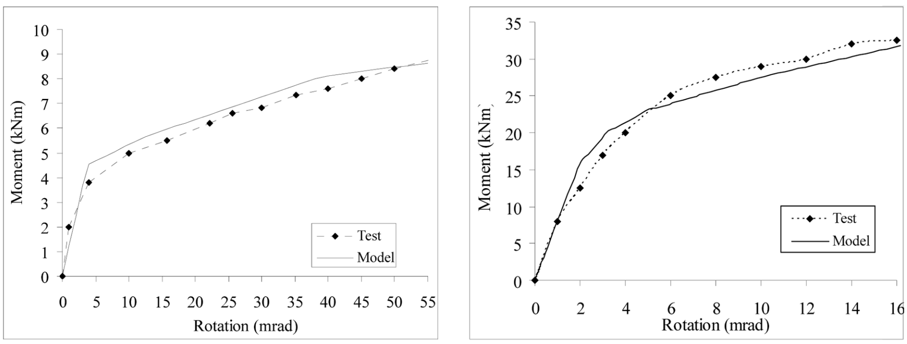

(a) Davison, *et al.* 1987 test (b) Yang and Lee 2007 test

Fig. 11 Double web angle connection at ambient temperature

(which are not included in the model). In addition, other general inaccuracies in the overall shape of the curves are attributed to the tri-linear idealisation in the model of the nonlinear response of individual components, and possible discrepancies in material and geometric properties.

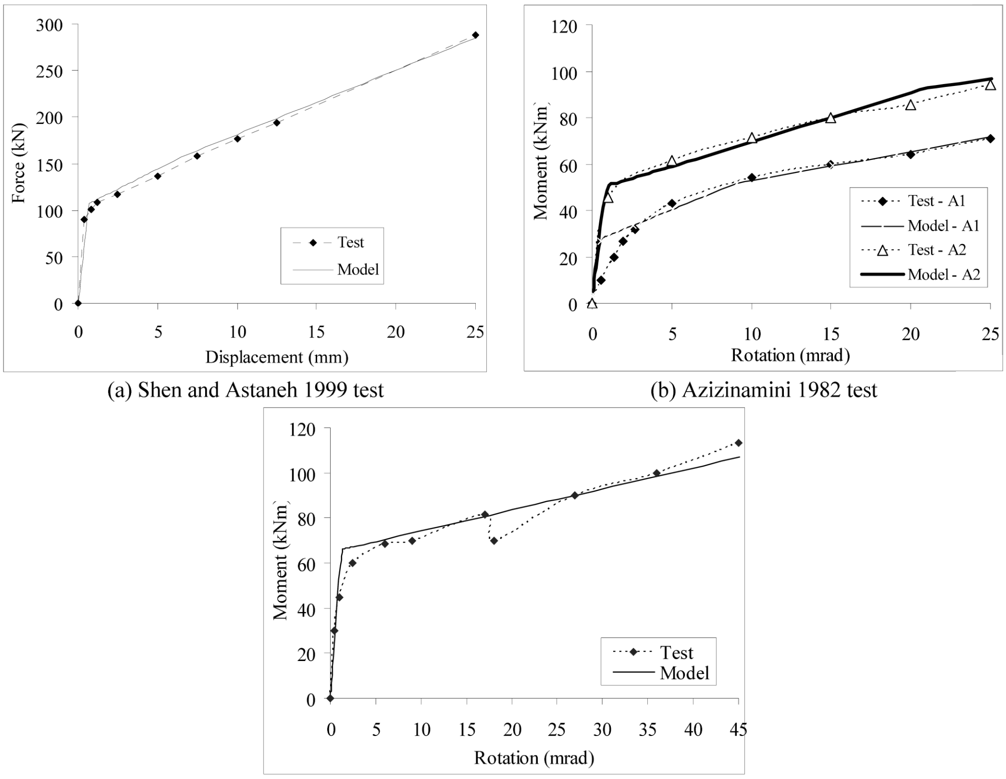

(a) Shen and Astaneh 1999 test

(b) Azizinamini 1982 test

(c) Kumoro, *et al.* 2004 test

Fig. 12 Top and seat angles connection at ambient temperature

4.2 Behaviour at elevated temperature

More studies on the response of various connection types at elevated temperature are becoming available in the literature. For T-stub components at elevated temperature, results from Specimens AA1 and AB1 tested by Spyrou, *et al*. (2004b) are used herein for validation of the model. As shown in Fig. 14, the initial stiffness and the yield capacity closely match the experimental results, indicating that the model is able to predict the behaviour of a T-stub component at elevated temperature based on degradation of material properties. It is noteworthy that this specimen behaves according to Mode 1.

For flush endplate connections, the experimental results of Al-Jabri, *et al*. (2004) are utilised for validation. The results are compared in Figs. 15 and 16 for isothermal and anisothermal response, respectively. Good agreement between the test results and the numerical simulations is observed. For the isothermal case, uniform temperature distribution within the joint is assumed since the variation of temperature profile given in the test is only 2% between the top and bottom beam flanges. At temperatures above 500°C, the accuracy of the connection stiffness cannot be adequately assessed due to lack of data captured in the test. For the anisothermal case with various initial moment values, the model can predict the test results accurately at lower temperature for all level of loading. However, as the temperature increases, slight differences are observed, particularly for higher moments. This is mainly attributed to the approximation of material properties with temperature variation.

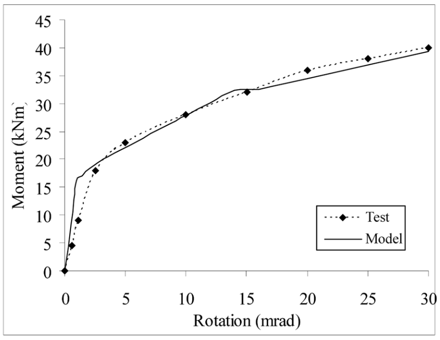

(a) 8S1

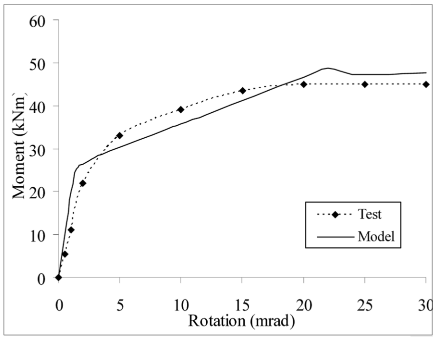

(b) 8S2

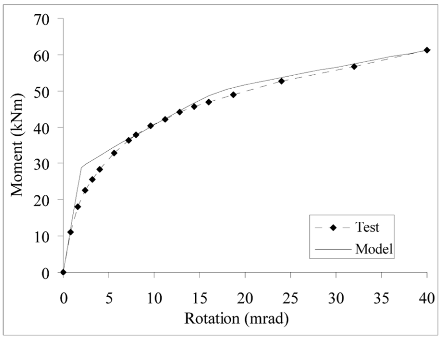

(c) 8S9

Fig. 13 Top-seat-web angles connections (Azizinamini, *et al*. 1987)

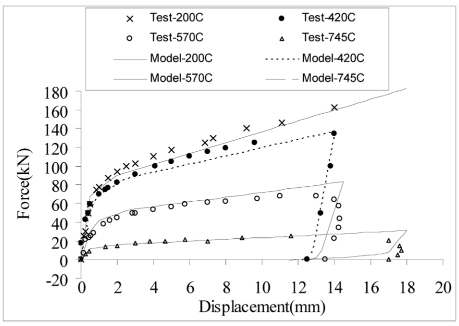

(a) Test AA1

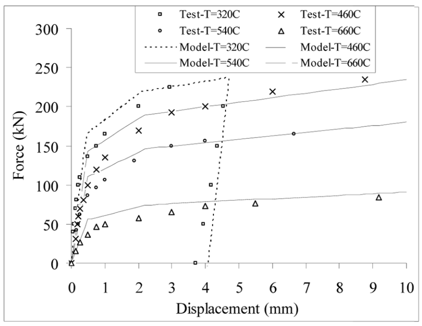

(b) Test AB1

Fig. 14 T-stub at elevated temperature (Spyrou, *et al*. 2004b)

For extended endplate connections, experimental results from Qian, *et al*. (2008) and Wang, *et al*. (2007) are considered. Isothermal behaviour of the connection at three temperature loadings (i.e. 400, 550 and 700^{o}C) is shown in Fig. 17. It is evident that the model can predict the stiffness accurately, but the ultimate moment capacity is may be slightly underestimated. For the anisothermal case, depicted in Fig. 18, the model cannot capture the rotation accurately at the lower temperature range. It should be noted that this connection is located in a single joint, where the contribution of the shear panel may be significant. Since this was not considered the simulation, it may result in a higher stiffness of the joint

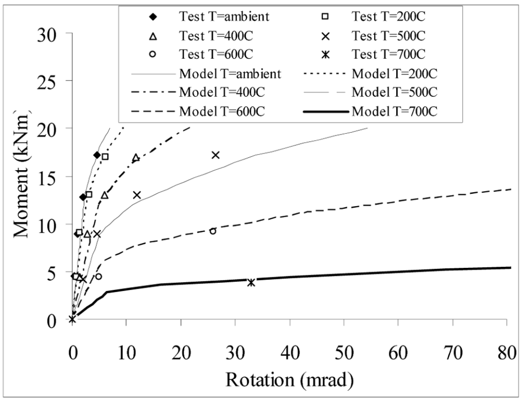

Fig. 15 Isothermal behaviour for flush endplate connections (Al-Jabri, *et al.* 2005)

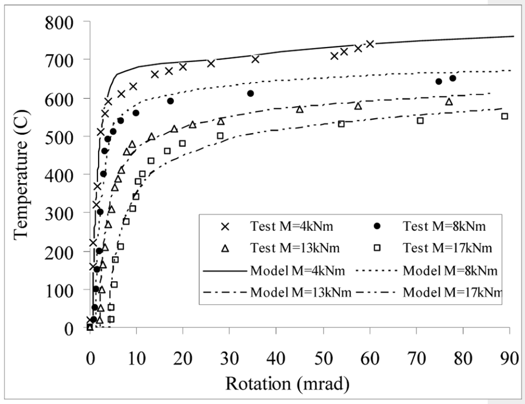

Fig. 16 Anisothermal response for flush endplate connections (Al-Jabri, *et al.* 2005)

compared to the test result.

In the case of top-seat angles and combined top-seat-web angles, whereas the ultimate capacity is predicted reasonably well, there is significant discrepancy between the initial stiffness predicted by the analysis and that obtained in tests under anisothermal loading, as shown in Fig. 19. This indicates the need for additional validation of the model representing angle connections with a wider set of experimental results which is currently lacking in the literature, and which may result in further model refinement.

Table 2 summarises the comparison of initial stiffness and resistance between the numerical and experimental results under isothermal loading. Only T-stub and endplate connections are tabulated as experimental results for angle connections under isothermal loading are lacking. It can be observed that both the initial stiffness and resistance are reasonably predicted by the model with a percentage error less than 15% and 27%, respectively.

Investigation of the connection response within a sub-frame under fire is based herein on the recent experimental work by Santiago, *et al.* (2009). Only bolted flush and extended endplate are considered.

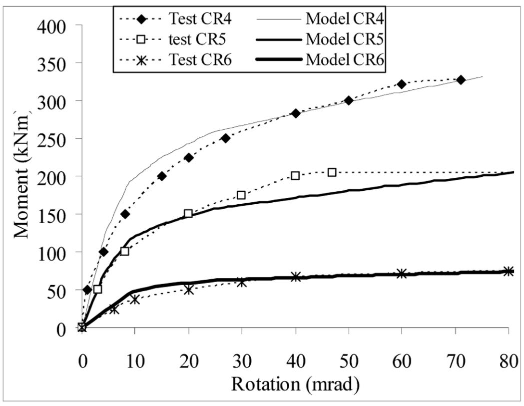

Fig. 17 Isothermal behaviour for extended endplate connections (Qian, *et al.* 2008)

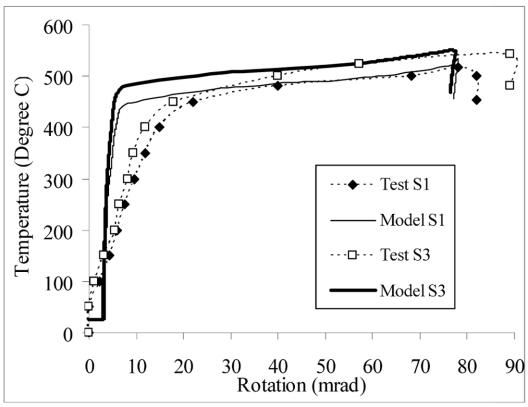

Fig. 18 Anisothermal response for extended endplate connections (Wang, *et al.* 2007)

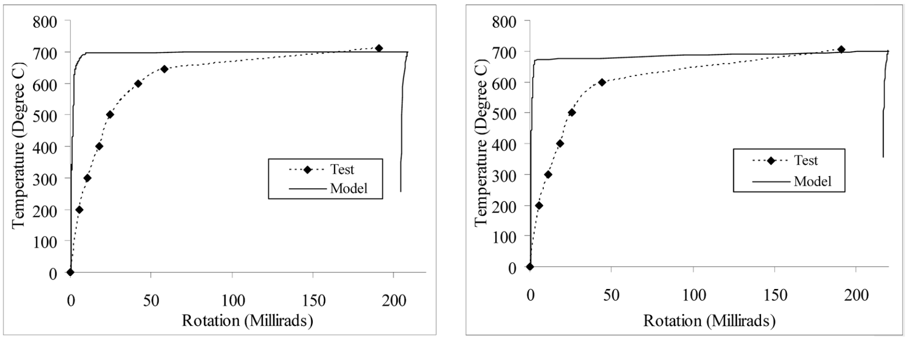

Test S1 Test S2

Fig. 19 Anisothermal response for top-seat and top-seat-web angle connections (Saedi Daryan and Yahyai 2009)

The results are presented in the form of mid-span deflection of the beam against time for four connection typologies, as shown in Fig. 20. The actual connection temperatures recorded in the test are applied in the model. At lower temperatures (T < 25 min), the model predicts the actual response accurately. Beyond T = 25 min (Temperature > 550ºC), the beam deflects rapidly due to the reduction of strength and stiffness. This behaviour can be predicted accurately by the model, except for extended

Table 2 Comparison between the numerical and experimental results in the prediction of initial stiffness and resistance for isothermal loading

Connection	Author	Initial Stiffness			Force / Moment resistance		
		Numerical (kN/mm)	Experimental (kN/mm)	% error	Numerical (kN)	Experimental (kN)	% error
T-stub	Spyrou, *et al*. -AA1-200	104.40	104.40	0.00	83.49	87.07	4.11
	Spyrou, *et al*. -AA1-420	104.40	104.40	0.00	78.64	73.27	–7.32
	Spyrou, *et al*. -AA1-570	77.78	85.00	8.50	47.95	46.19	–3.82
	Spyrou, *et al*. -AA1-745	23.20	23.20	0.00	14.50	14.51	0.03
	Spyrou, *et al*. -AB1-320	373.75	374.38	0.17	207.25	189.54	–9.34
	Spyrou, *et al*. -AB1-460	286.00	307.00	6.84	180.82	173.52	–4.20
	Spyrou, *et al*. -AB1-540	220.00	232.00	5.17	139.51	140.42	0.65
	Spyrou, *et al*. -AB1-660	111.80	117.00	4.44	70.71	65.39	–8.13
		Numerical (kNm/rad)	Experimental (kNm/rad)	% error	Numerical (kNm)	Experimental (kNm)	% error
Flush endplate	Al-Jabri, *et al*. -amb	5649.72	6162.46	8.32	15.26	15.10	–1.07
	Al-Jabri, *et al*. -200	5714.29	6162.46	7.27	12.01	10.89	–10.30
	Al-Jabri, *et al*. -400	2651.52	3079.08	13.89	14.24	11.36	–25.36
	Al-Jabri, *et al*. -500	1769.91	2100.00	15.72	13.67	11.05	–23.74
Extended endplate	Qian, *et al*. -CR4	28501.23	28642.86	0.49	235.94	232.73	–1.38
	Qian, *et al*. -CR5	16840.58	16666.67	–1.04	144.74	198.19	26.97
	Qian, *et al*. -CR6	4305.79	4166.67	–3.34	65.87	63.44	–3.83
Mean error				4.429			–4.449
Standard deviation				5.563			11.651

endplate test EJ01, for which the model slightly overestimates the actual beam response. This might be related to inaccuracies in the assumed material properties of the connection at elevated temperature. During the cooling stage, the connection is subjected to tension, which causes yielding of the endplate component in bending, represented as a plateau in the curves.

Overall, the validation studies described in this section demonstrate the general accuracy and reliability of the proposed models, although they point to the need for further validation and refinement in some cases. The models are capable of capturing the main response characteristics of a number of typical connection configurations under ambient and elevated temperature conditions, including the possible influence of load reversal.

5. Conclusions

A component-based temperature-dependent connection model was proposed in this paper. The proposed model was implemented within the finite element program, ADAPTIC. The model is capable of representing the nonlinear temperature-dependent response of five connection types under generalised loading conditions including possible load reversals. The approach is consistent with the principles adopted in Eurocode 3 Part 1-8. Validation against available experimental results at ambient and elevated temperature was carried out. At ambient temperature, close prediction of the key parameters

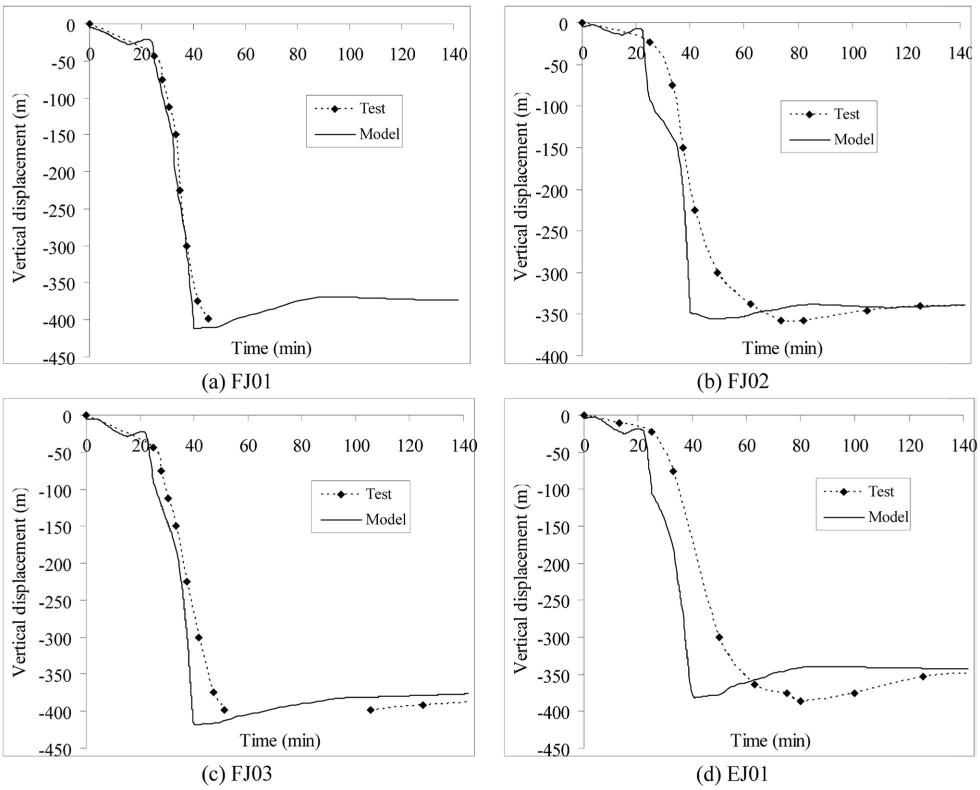

Fig. 20 Mid-span deflection of the beam in a sub-frame (Santiago, *et al.* 2009)

within the force-deformation or moment-rotation response was obtained for all connection types. At elevated temperature, the analytical simulations also provided a faithful representation of the experimental results, particularly for endplate connections considered as either isolated joints or incorporated within structural sub-frames. For angle connections, although there was good agreement between the analysis and tests, there is room for further investigation of the behaviour and refinement of the model in order to capture the influence of active components at elevated temperature more accurately. In general, some discrepancies between the experimental results and numerical simulations were observed. These are largely attributed to inevitable inaccuracies in defining the temperature-dependant material properties, in addition to other factors which are not covered in the model such as bolt slippage, residual stresses and imperfections. Overall, this investigation highlights the need for further experimental studies on the response of connections at elevated temperature, particularly angle configurations, in order to provide data for additional validation, calibration and refinement of the suggested models.

References

Al-Jabri, K.S., Burgess, I.W. and Plank, R.J. (2004), "Prediction of the degradation of connection Characteristics at elevated temperature", *J. Constr. Steel Res*., **60**, 771-781.

Al-Jabri, K.S., Burgess, I.W. and Plank, R.J. (2005), "Spring-stiffness model for flexible end-plate bare-steel joints in fire", *J. Constr, Steel Res*., **61**(12), 1672-1691.

Azizinamini, A. (1982), *Monotonic response of semi-rigid steel beam to column connections*, M.S. thesis, Columbia, University of South Carolina.

Azizinamini, A., Bradburn, J.H. and Radziminski, J.B. (1987), "Initial stiffness of semi-rigid steel beam-to-column connections", *J. Constr. Steel Res.*, **8**, 71-90.

Bailey, C.G., Burgess, I.W. and Plank, R.J. (1996), "Analyses of the effects of cooling and fire spread on steelframed buildings", *Fire Safety J*., **26**, 273-279.

Bailey, C.G., Lennon, T. and Moore, D.B. (1999), "The behaviour of full-scale steel-framed buildings subjected to compartment fires", *Struct. Eng*., **77**(8),15-21.

Block, F.M., Burgess, I.W., Davison, J.B. and Plank, R.J. (2007), "The development of a component-based connection element for endplate connections in fire", *Fire Safety J.*, **42**(6-7), 498-506.

Davison, J.B., Kirby, P.A. and Nethercot, D.A. (1987), "Rotational stiffness characteristics of steel beam-to-column connections", *J. Constr. Steel Res*., **8**, 17-54.

De Lima, L.R.O., Simoes Da Silva, L., Da S. Vellasco, P.C.G. and De Andrade, S.A.L. (2004), "Experimental evaluation of extended endplate beam-to-column joints subjected to bending and axial force", *Eng. Struct*., **26**(10), 1333-1347.

El-Rimawi, J.A., Burgess, I.W. and Plank, R.J. (1996), "The treatment of strain reversal in structural members during the cooling phase of a fire", *J. Constr. Steel Res*., **37**(2),115-35.

European Committee for Standardisation (2005), *EN 1993-1-8: 2005: Design of Steel Structures*, Part 1-8: Design of Joints, Brussels.

Faella, C., Piluso, V. and Rizzano, G. (2000a), *Cyclic behaviour of bolted t-stubs: experimental analysis and modelling*, in Behaviour of Steel Structures in Seismic Areas, Mazzolani & Tremblay, eds., Balkema, Rotterdam, 183-190.

Faella, C., Piluso, V. and Rizzano, G. (2000b), *Structural steel semi rigid connection: Theory, Design and Software*, CRC Press LLC.

Girao Coelho, A.M., Bijlaard, F.S.K. and Simoes da Silva, L. (2004), "Experimental assessment of the ductility of extended endplate connections", *Eng. Struct*., **26**, 1185-1206.

Hongxia, Y., Burgess, I.W., Davison, J.B. and Plank, R.J. (2009a), "Tying capacity of web cleat connections in fire, Part1: Test and finite element simulation", *Eng. Struct*., **31**(3), 651-663.

Hongxia, Y., Burgess, I.W., Davison, J.B. and Plank, R.J. (2009b), "Experimental investigation of the behaviour of fin plate connections in fire", *J. Constr. Steel Res*., **65**, 723-736.

Izzuddin, B.A. (1991), *Nonlinear dynamic analysis of framed structures*, PhD Thesis, Imperial College of Science, Technology and Medicine, London.

Kirby, B.R. (1995), "The behaviour of high-strength grade 8.8 bolts in fire", *J. Constr. Steel Res*., **33**(1-2), 3-38.

Komuro, M., Kishi, N. and Chen, W.F. (2004), "Elasto-plastic FE analysis on moment-rotation relations of top-andseat angle connections", 5th *Int. Workshop on Connections in Steel Structures: Behaviour, strength and design*, Faculty of Civil Engineering and Geosciences of the Delft University of Technology.

Krawinkler, H., Bertero, V.V. and Popov, E.P. (1975), "Shear behaviour of steel frame joints", *J. Struct. Div. ASCE*, **101**(No. ST11), 2317-2336.

Lawson, R.M. (1990), "Behaviour of steel beam-to-column connections in fire", *Struct. Eng*., **68**(1417), 263-271.

Leston-Jones, L.C., Burgess, I.W., Lennon, T. and Plank, R.J. (1997), "Elevated-temperature moment-rotation tests on steelwork connections", *Proc. of the Institution of Civil Engineers: Structures and Buildings*, **122**(4), 410-419.

OConnor, M.A., Kirby, B.R. and Martin, D.M. (2003), "Behaviour of a multi-storey steel framed building in fire", *Struct. Eng*., **81**, 27-36.

Qian, Z.H., Tan, K.H. and Burgess, I.W. (2008), "Behavior of steel beam-to-column joints at elevated temperature: Experimental investigation", *J. Constr. Steel Res*., **34**(5), 713-26.

Qian, Z.H., Tan, K.H. and Burgess, I.W. (2009), "Numerical and analytical investigations of steel beam-to-column joints at elevated temperatures", *J. Constr. Steel Res*., **65**, 1043-1054.

Ramli Sulong, N.H. (2005), *Behaviour of steel connections under fire conditions*, PhD thesis, Imperial College London, University of London.

Ramli Sulong, N.H., Elghazouli, A.Y. and Izzuddin, B.A. (2007), "Behaviour and design of of beam-tocolumn connections under fire conditions", *Fire Safety J*., **42**, 437-451.

Saedi Daryan, A. and Yahyai, M. (2009),"Behavior of bolted top-seat angle connections in fire", *J. Constr. Steel Res*., **65**, 531-541.

Santiago, A., Da Silva, L.S., Real, P.V., Vaz, G. and Lopes, A.G. (2009), "Experimental evaluation of the influence of connection typology on the behavior of steel structures under fire", *Eng. J*., **46**(2), 81-98.

Shen, J. and Astaneh-Asl, A. (1999), "Hysteretic behavior of bolted-angle connections", *J. Constr. Steel Res*., **51**(3), 201-218.

Simoes Da Silva, L., De Lima, L.R.O., Da S. Vellasco, P.C.G. and De Andrade, S.A.L. (2004), "Behaviour of flush endplate beam-to-column joints under bending and axial force", *Steel Compos. Struct*., **4**(2),77-94.

Simoes da Silva, L., Santiago, A. and Vila Real, P. (2001), "A Component Model for the Behaviour of Steel Joints at Elevated Temperatures", *J. Constr. Steel Res*., **57**(11), 1169-1195.

Simoes da Silva, L., Santiago, A., Vila Real, P. and Moore, D. (2005), "Behaviour of steel joints under fire loading", *Steel Compos. Struct.*, **5**(6), 485-513.

Spyrou, S., Davison, J.B., Burgess, I.W. and Plank, R.J. (2004a), "Experimental and analytical investigation of the compression zone component within a steel joint at elevated temperatures", *J. Constr. Steel Res.*, **60**(6), 841-865.

Spyrou, S., Davison, J.B., Burgess, I.W. and Plank, R.J. (2004b), "Experimental and analytical investigation of the tension zone components within a steel joint at elevated temperatures", *J. Constr. Steel Res*., **60**(6), 867-896.

Wang, W.Y., Li, G.Q. and Dong, Y.L. (2007), "Experimental study and spring-component modelling of extended end-plate joints in fire", *J. Constr. Steel Res*., **63**, 1127-1137.

Weynand, K., Jaspart, J.P. and Steenhuis, M. (1995), "The stiffness model of revised annex", *J. Eurocode 3*, Connections in steel structures: Behaviour, strength and design, Trento, Italy, 441-452.

Yang, J.G. and Lee, G.Y. (2007), "Analytical models for the initial stiffness and ultimate moment of a double angle connection", *Eng. Struct*., **29**, 542-551.

DN